Thermodynamic modeling and composition design for the formation of Zr–Ti–Cu–Ni–Al high entropy bulk metallic glasses

ARTICLE *in* INTERMETALLICS · OCTOBER 2015

Impact Factor: 2.13 · DOI: 10.1016/j.intermet.2015.04.007

3 AUTHORS, INCLUDING:

Satish Idury
Visvesvaraya National Institute of Technology
7 PUBLICATIONS **10** CITATIONS
SEE PROFILE

Jatin Bhatt
Visvesvaraya National Institute of Technology
45 PUBLICATIONS **211** CITATIONS
SEE PROFILE

Intermetallics 65 (2015) 42–50

Contents lists available at ScienceDirect

Intermetallics

journal homepage: www.elsevier.com/locate/intermet

Thermodynamic modeling and composition design for the formation of Zr–Ti–Cu–Ni–Al high entropy bulk metallic glasses

K.S.N. Satish Idury [a, *], B.S. Murty [b], Jatin Bhatt [a]

[a] Department of Metallurgical and Materials Engineering, Visvesvaraya National Institute of Technology, Nagpur, 440 010, India
[b] Department of Metallurgical and Materials Engineering, Indian Institute of Technology Madras, Chennai, 600 036, India

ARTICLE INFO

Article history:
Received 5 December 2014
Received in revised form
2 March 2015
Accepted 10 April 2015
Available online 6 June 2015

Keywords:
A. High–entropy alloys
A. Metallic glasses
B. Alloy design
B. Glass forming ability
E. Phase stability, prediction

ABSTRACT

This work explores the idea of predicting metallic glass forming composition in a multi component alloy for which an equilibrium phase diagram is yet to be deciphered. Deep eutectic regions in a quaternary alloy (Zr–Ti–Cu–Ni) have been extrapolated to the quinary Zr–Ti–Cu–Ni–Al system for designing a potential bulk glass forming composition. P_{HSS} parameter which is the product of mixing enthalpy, mismatch entropy and configurational entropy of an alloy, has been utilized for thermodynamic modeling. P_{HSS} values are computed through substitution of Al into the each of the fifteen quaternary eutectics that have been reported in the literature in the Zr–Ti–Cu–Ni system. A good correlation of P_{HSS} range between modeled alloys and established glass formers indicates the subtle efficacy of this method for high entropy amorphous alloy design through a rationale thermodynamic approach.

1. Introduction

The concept that metallic alloys can form glasses has been introduced in the year 1959 after the splat quenching experiment on an Au–Si alloy by Pol Duwez [1]. Despite active research over the years on the nature of glass transition phenomenon and the atomic structure of the metallic glass (MG), a consensus in the scientific community as to how the atomic structure of glass influences macroscopic properties is still elusive. However, it has been accepted that MGs possess dense random packing of atoms with metallic bonding [2]. As a result of this structure, dislocations and grain boundaries are nonexistent thereby imparting enhanced physical and chemical properties to MGs [3]. In addition to superior functional and structural properties, the ability to thermo plastically engineer them into intricate shapes renders glass forming alloys the ideal choice for micro electro mechanical systems and biological implant applications [4]. In view of this interesting combination of superior mechanical properties and processability, discovering novel bulk glass formers in multi component alloy systems is a widely pursued research area in materials science.

Significant number of glass forming alloys has been reported till date in various alloy systems based on certain empirical rules [5]. Most of these alloys have one or two major elements and rest of the elements are alloyed to give the compositions near binary and ternary deep eutectics through substitution of like elements in the periodic table. The alloying is attributed to effectively bond the secluded atomic clusters and result in formation of large network which acts as barrier for atomic rearrangements [6]. The success of this method is attributed to the reliable knowledge that was acquired over the years on phase diagrams in binary and ternary alloy systems. However, to identify new glass forming compositions in quaternary and higher order systems, limited thermodynamic data is available pertaining to deep eutectic compositions of these alloys. To obviate these lacunae, Zhao et al. [7] demonstrated for the first time as to how high entropy concept can be applied to design a reliable MG former that exhibits remarkable deformation characteristics at room temperature and provided a new pathway to explore BMGs with optimal GFA. In a recent review on HEBMGs, it was opined that high mixing entropy renders amorphous phase formation easier than conventional alloy systems [8]. Based on the high mixing entropy alloying principle, various research groups successfully casted equiatomic BMG alloys of various critical diameters [9–11] in different alloy systems. Among those alloys, equiatomic TiZrHfCuNiBe [10] that has been reported to from BMG with critical diameter of 15 mm is the largest obtained till to date.

* Corresponding author. Tel.: +91 7387896851.
E-mail address: satishidury@gmail.com (K.S.N. Satish Idury).

http://dx.doi.org/10.1016/j.intermet.2015.04.007
0966-9795/

The effective synthesis of HEBMGs with large GFA render credibility to the hypothesis that the large configurational entropy obtained due to equal concentration of elements stabilizes super cooled liquid through lowering the temperature of the eutectic point [11]. Hence, designing amorphous alloys by alloying elements in near equiatomic concentrations has the potential to yield bulk glass formers in multi component systems where phase diagrams do not reveal deep eutectics.

However, Zhang et al. [12] have demonstrated that phase stability in a HEA is governed by Gibbs free energy which contains contributions from enthalpy and entropy. Mixing elements in equal concentration will result in a phase that has the largest entropy of mixing but may not necessarily result in lowering Gibbs free energy of that specific phase [12]. Moreover, there exists reports in literature indicating that equiatomic alloys do form intermetallic phases [13] substantiating the report of Zhang et al. [12]. Hence, while resorting to designing MGs through HEA view point one needs an explicit thermodynamic criterion that incorporates enthalpy and entropy terms to predict glass formation.

The combination of mixing enthalpy (ΔH_{mix}) and topological parameter ($\Delta S_\sigma/k_B$), which measure the strength of chemical interactions and entropy generated due to atomic size mismatch of an alloy respectively, are among thest successful thermodynamic criteria that enabled prediction of glass formation in a multitude of alloy systems [5,14]. Yun et al. [15] established through molecular dynamics simulations that optimized window of atomic size difference and heat of mixing are critical prerequisites for glass formation. Takeuchi et al. [16] demonstrated the effectiveness of chemical and topological parameters in stabilizing glass formation through extensive studies on various ternary amorphous alloy systems. The above report by Takeuchi et al. [16] identified the two exclusive regions bounded by chemical and topological parameters in a two dimensional plot, in which amorphous phase and solid solution phases form. In a following report, Takeuchi et al. [17] captured the statistical data of mixing enthalpy (ΔH_{mix}) and atomic size difference parameter (δ) of huge number of quinary to ten component equiatomic alloy systems in two dimensional plot of ΔH_{mix} versus δ and reported that identifying the window of chemical and topological parameters for equiatomic alloys, is a promising method for designing HEAs and high entropy bulk metallic glasses (HEBMGs). In separate reports, Yang and Zhang [18] and Guo et al. [19] reported similar sort of two parameter scheme that represent phase selection mechanism between amorphous phase and solid solution phase in HEAs.

Taking cues from the above literature, in current paper new HEBMG compositions (alloys in proximity to high configurational entropy regime though they are not perfectly equiatomic) are designed in Zr–Ti–Cu–Ni–Al system through identification of the range of chemical and topological parameters that resulted in BMG formation for certain alloys in this quinary system, as earlier reported by various groups. The chemical and topological parametric values of the modeled alloys that overlap with the experimentally proven BMGs in this quinary system are proposed to be the new HEBMG compositions.

2. Modeling methodology

Fifteen quaternary eutectic compositions in Zr–Ti–Cu–Ni system (Table 1 – Table 15 in supplementary data) [20,21] are used as the starting points for thermodynamic modeling. Each of these compositions is designated serially as E1–E15 in the present work. For each quaternary eutectic composition Al is substituted up to 20 at % through successive increment of 5 at % at a time in two ways. In the first case, in each of the compositions in E1–E15 alloys, the major element is substituted with Al and hence forth this is referred to as mode I substitution. In the second way, Al is substituted such that it results into change in the composition of all constituent elements and is referred to as mode II substitution in subsequent discussion. For example, in case of E1 the Al substituted compositions are: $Zr_{46.6-x}Ti_{14.2}Cu_{13.8}Ni_{25.4}Al_x$ (Mode I substitution) and $(Zr_{46.6}Ti_{14.2}Cu_{13.8}Ni_{25.4})_{1-x}Al_x$ (Mode II substitution) where (x = 5, 10, 15 and 20). The substitution of Al in E1-E15 as described above resulted in 120 quinary compositions for which P_{HSS} values are calculated (provided as supplementary data).

The description about P_{HSS} and the associated calculation procedure is enumerated in subsequent section. The rationale behind substituting quaternary compositions in the above two modes is to sample more number of alloys in vast compositional range of Zr–Ti–Cu–Ni–Al system. As the reported eutectics in Zr–Ti–Cu–Ni comprise of Zr, Ti, Cu and Ni rich alloys, substituting in this manner guaranteed that the alloys representing the entire spectrum of the compositional region in this quinary system are considered for thermodynamic calculations. Also, by substituting the major element in each of the eutectic composition it is strived to attain near equiatomic concentration of the elements. It is pertinent to mention that none of the alloy compositions obtained on substitution of Al is equiatomic. However, they are referred to as HE compositions in the present work since their configurational entropy is high (refer to $\Delta S_c/R$ values in Table1 – Table 15 of supplementary data). The motivation behind adopting this modeling procedure is twofold. First, restriction of compositional optimization near to quaternary eutectic points ensures high probability for glass formation in quinary alloys. Second, it has been reported that doping with Al enhances the spatial connectivity and increases the population of icosahedral clusters as a result of increased electron interactions and bond shortening in Zr–Cu binary alloy [22]. Since Zr–Ti–Cu–Ni alloy can be regarded as pseudo-binary Zr–Cu alloy system, it is envisaged that bulk glass formation can be realized in similar manner due to doping Al in Zr–Ti–Cu–Ni system.

3. Thermodynamic and topological parameters calculations

3.1. Enthalpy of chemical mixing

Enthalpies of chemical mixing (ΔH_{mix}) are obtained from Miedema's methodology. Miedema's method has been successful to predict the formation enthalpies of alloys that can be further utilized to develop Gibbs free energy–composition diagrams to predict the thermodynamic stability of glasses. This method has been developed initially for binary systems. Later the same principle has been extended for many ternary systems by Gallego et al. [23] and Murty et al. [24]. However, the report by Murty et al. [24] in ternary Ti–Ni–Cu system is the first attempt to calculate glass forming range and correlate it with mechanical alloying experimental results for concentrated solutions, as against Gallego et al. [23] who restricted their work to dilute solutions. The Miedema's methodology is based on the premise that the electron reorganization generated at the interface between the dissimilar atomic cells will result in enthalpy upon alloying [25]. In the mixing enthalpy calculations, the ΔH_{mix} for an alloy is obtained by the summation of the individual binaries in the quinary system. The enthalpies are arrived at through the procedure reported by Takeuchi and Inoue [26]. As per this model, ΔH_{mix} for a ternary system is given by

$$\Delta H_{chem(ABC)} = \Delta H^c_{AB} + \Delta H^c_{BC} + \Delta H^c_{AC} \quad (1)$$

$$\text{where } \Delta H^{c}_{AB} = 4\left[\sum_{k=0}^{3} \Omega_k (c_A - c_B)^k\right] c_A c_B \tag{2}$$

where Ω_k ($k = 0, 1, 2, 3$) is the approximation of ΔH_{mix} using the sub regular solution model and is an interaction parameter. c_A, c_B is the composition of A and B elements respectively.

3.2. Mismatch entropy

Mismatch entropy is calculated through the misfit term of Percus-Yevik integral equation, reported by Mansoori et al. [27]. It is a measure of randomness caused due to variation in atomic diameters of constituent atoms considering as hard spheres.

$$S_\sigma = k_B\left[\frac{3}{2}\left(\varsigma^2 - 1\right)y_1 + \frac{3}{2}(\varsigma - 1)^2 y_2 - \left\{\frac{1}{2}(\varsigma - 1)(\varsigma - 3) + \ln \varsigma\right\}(1 - y_3)\right] \tag{3}$$

k_B is Boltzmann's constant and parameter ζ is defined as $\zeta = 1/(1-\xi)$ and ξ is the packing fraction. ξ is taken as 0.64, implying dense random packing of the atoms. Dimensionless parameters y_1, y_2, y_3 are related by $y_1+y_2+y_3 = 1$ and are computed by the following equations.

$$y_1 = \frac{1}{\sigma^3}\sum_{j>i=1}^{3} (d_i + d_j)(d_i - d_j)^2 c_i c_j \tag{4}$$

$$y_2 = \frac{\sigma^2}{(\sigma^3)^2}\sum_{j>i=1}^{3} d_i d_j (d_i - d_j)^2 c_i c_j \tag{5}$$

$$y_3 = \frac{(\sigma^2)^3}{(\sigma^3)^2} \tag{6}$$

$$\sigma^k = \sum_{i=1}^{3} c_i d_i^k \ (k = 2, 3) \tag{7}$$

In the above equations d_i, d_j and c_i, c_j are the atomic diameters and compositions of i^{th} element and j^{th} element in the alloy respectively. The atomic diameters are obtained from Ref. [28].

3.3. Configurational entropy

Configurational entropy is a function of concentration of each constituting element of the alloy system.

$$\Delta S_{config} = -R\sum_{i=1}^{n} c_i \ln c_i \tag{8}$$

Here c_i is the composition of ith element in the alloy.

3.4. P_{HSS} parameter

This parameter has been proposed by Rao et al. [29] and is defined as the product of mixing enthalpy (ΔH_{mix}), normalized mismatch entropy ($\Delta S_\sigma/k_B$) and normalized configurational entropy ($\Delta S_c/R$) of an alloy composition. This is based on Inoue's criteria for glass formation. In this paper towards P_{HSS} computation, ΔH_{mix} is obtained through Takeuchi approach [26] as against Gallego approach adopted for calculation of ΔH_{mix} reported earlier [23].

4. Experimental details

In order to verify the glass formation predictive capability of the P_{HSS} model, four different alloys that were predicted to be HEBMG formers were synthesized through mechanical alloying. High energy ball milling for 9 h has been carried out in Fritsch Pulverisette P-5 planetary ball mill (Fritsch GmbH, Idar-Oberstein, Germany) for $Zr_{43.5}Ti_{7.6}Cu_{30.4}Ni_{8.5}Al_{10}$ (Z1) of QE3, $Zr_{40.3}Ti_{4.6}Cu_{34.1}Ni_{11}Al_{10}$ (Z2) of QE2, $Zr_{15.2}Ti_{37.4}Cu_{10.4}$ $Ni_{27}Al_{10}$ (T1) and $Zr_{14.4}Ti_{45.1}Cu_{9.9}$ $Ni_{25.6}Al_5$ (T2) of QE9 alloy compositions with tungsten carbide (WC) as milling media. The experiment was carried out at 300 rpm in wet condition through toluene medium with ball to powder ratio of 10:1. Elemental powder blends of Zr, Ti, Cu, Ni and Al of 99%, 98%, 99.5%, 99.5% and 98% purity respectively were utilized for mechanical alloying. After milling for every three hours the alloyed powders have been characterized for phase formation using X-Ray diffraction (XRD) using PANalytical X'pert-Pro diffractometer (PANalytical B.V. Almelo, Netherlands) with Cu K_α ($\lambda = 0.1542$ nm) radiation.

5. Results and discussion

5.1. Modeling results

The ΔH_{mix} is plotted against concentration of Al for the quinary Zr–Ti–Cu–Ni–Al alloys in Fig. 1a (mode I substitution) and Fig. 1b (mode II substitution). As many of the ΔH_{mix} values overlap in both the modes at each QE (Table 1–Table 15 of supplementary data), separate graphs are plotted for each of the mode for better illustration of trend in data. Furthermore, the same methodology is adopted to represent trend in mismatch entropy (Fig. 2a and Fig. 2b) and configurational entropy (Fig. 4a and Fig. 4b) also. The legend QE1-QE15 represents the series of alloys obtained on substitution of Al in each quaternary eutectic composition.

The results of the thermodynamic calculations are appended in supplementary data. The two substitution modes resulted in minor variation in concentration of the respective constituent elements that led to deviations in their corresponding mixing enthalpies. However, the disparity in ΔH_{mix} is minimal and both the modes reflected similar trend in change of ΔH_{mix} with Al when all the QEs in two modes are compared simultaneously. The negative ΔH_{mix} is enhanced marginally with increment in % Al in almost all the QEs. The slope of negative ΔH_{mix} is the highest in QE 7 (Fig. 1a) among all quinary modeled alloys. In QE 7 series of alloys, Cu is the major alloying element and has the negative enthalpy of mixing of −7.6 kJ/mol [26] with Al, which is significantly less negative as compared to that of Zr, Ti and Ni with Al (−43.7, −29.5 and −22.3 kJ/mol respectively). Similar trend in decrease of ΔH_{mix} can also be observed in QE 1 in both the modes of substitution.

Substituting Al for Cu in QE 7 increased the chemical interaction between Al and other elements that led to the observed trend in Fig. 1a. QE 4, QE5 and QE 12 (Fig. 1a and b) are the series of alloys that exhibit largest negative enthalpy of mixing (<−35 kJ/mol) range. These three sequence of alloys are richer in Ni and Zr that has the ΔH_{mix} of −48.4 kJ/mol (Ni–Zr pair), the most negative among all the constituent binary pairs in this quinary alloy. It has been reported that [30] Zr_2Ni phase is the most competing phase with glass phase and GFA can be improved by decreasing the Ni concentration in this quinary alloy system through suppression of Zr_2Ni phase formation. Hence it can be regarded that ΔH_{mix} of −35 kJ/mol is a lower bound below which Zr_2Ni phase is preferable over amorphous phase. QE11 and QE 7 alloys are richer in Cu and Ti, having ΔH_{mix} greater than −20 kJ/mol. Cu has ΔH_{mix} of −8.9 kJ/mol with Ti that is significantly lower than −22.6 kJ/mol for (Zr–Cu pair) [26].

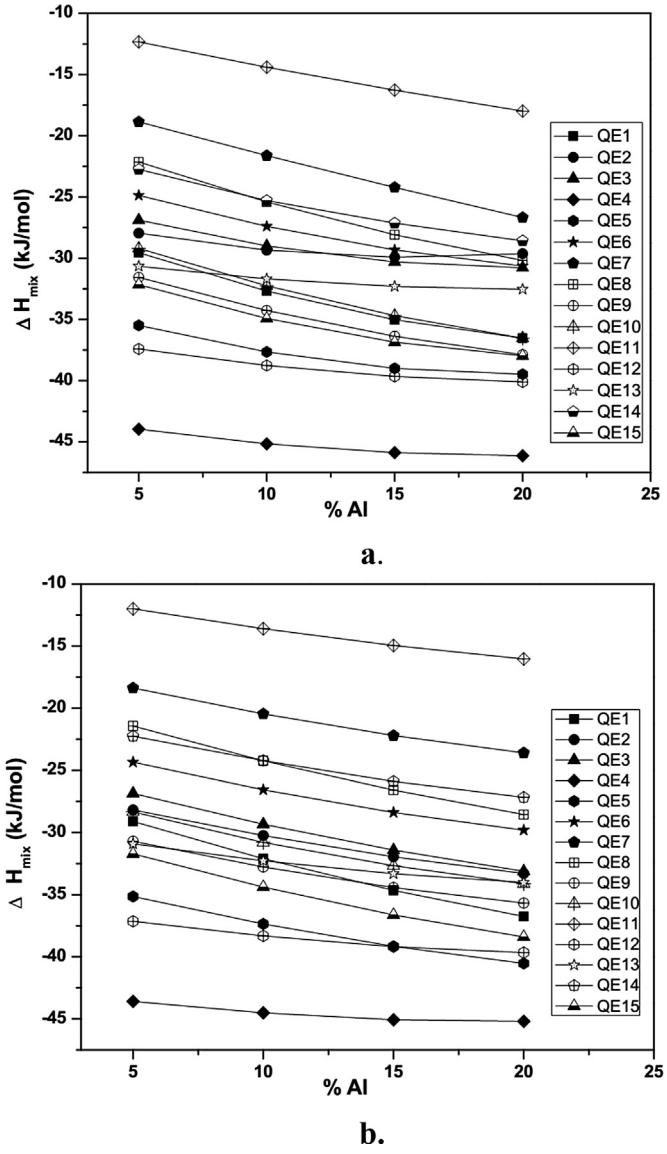

Fig. 1. Variation of ΔH_{mix} of quinary alloys with concentration of Al for (a) mode I and (b) mode II substitution.

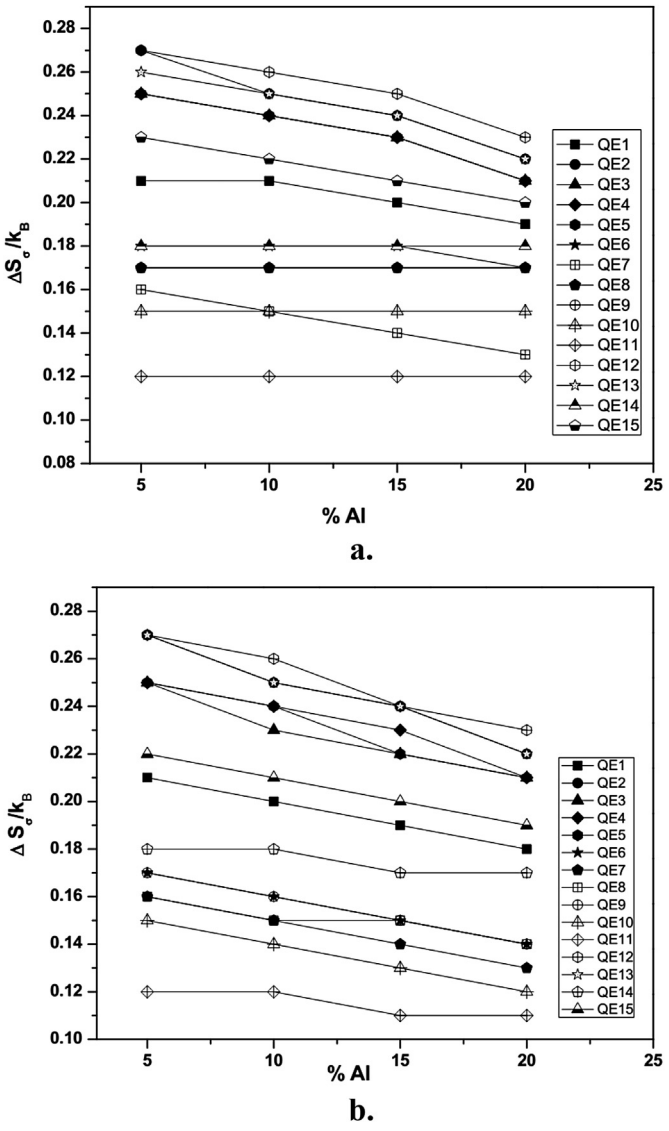

Fig. 2. Variation of $\Delta S_\sigma/k_B$ with concentration of Al for (a) mode I and (b) mode II substitution.

Cao et al. [31] reported that the best glass formers lie in Zr rich region of the Zr–Ti–Cu–Ni–Al system after comprehensive computational thermodynamic modeling of the entire quinary system. QE11 and QE 7 are much leaner in Zr and represent regions incompatible for glass formation due to less negative ΔH_{mix}. From the preceding discussion it can be inferred that the ΔH_{mix} range −35 to −20 kJ/mol can be a preliminary criteria to discern between amorphous phase and other phases. It is also evident from both the plots that most of the series of QEs are clustered between ΔH_{mix} range −33 to −27 kJ/mol. Hence one needs to resort to additional criteria in addition to ΔH_{mix} to discern the best glass formers from that population of alloys.

Fig. 2a and b represent the graphs of mismatch entropy ($\Delta S_\sigma/k_B$) against concentration of Al for all QEs in mode I and mode II substitution, respectively. In all the respective QEs no significant deviation in slope of $\Delta S_\sigma/k_B$ is observed with increment in Al concentration. It can be noted that all the QEs tend to be grouped into two distinct zones (Fig. 2a and b). One region represents the alloys that lie within $\Delta S_\sigma/k_B$ range (0.20–0.27), which are richer in either Zr and Ni or Zr and Cu concentrations. Another zone represents the alloys that lie within $\Delta S_\sigma/k_B$ range (0.11–0.18), which are rich in either Ti and Cu or Ti and Ni concentrations. QE 11 series alloys are richest in Cu concentration and they represent the lower bound of mismatch entropy in this quinary system (Fig. 2a and b). QE 12 series alloys are richer in Ni and represent the upper bound for mismatch entropy. It is also apparent from both the graphs (Fig. 2a and b) that, for alloys in region of higher mismatch entropy, Al addition leads to greater slope of decrease in $\Delta S_\sigma/k_B$.

However for certain compositions in QEs 9, 10, 11 and 14 that lie in region of lower mismatch entropy, $\Delta S_\sigma/k_B$ is almost constant with Al addition. Ti rich alloys comprise the $\Delta S_\sigma/k_B$(0.11–0.18) region, in which the atomic diameter of Ti is 0.2924 nm and that of Al is 0.2864 nm [28]. Since both the Ti and Al atoms have almost similar diameters, increase in Al concentration did not enhance entropy due to atomic size mismatch in these compositions (Fig. 2a and b). However for the case of compositions in the $\Delta S_\sigma/k_B$ range of 0.20–0.27 that are richer in either Zr and Ni or Zr and Cu, Al atoms are of intermediate size in comparison to Zr (0.3206 nm), Cu (0.2556 nm) [28]. Hence, addition of Al decreased the entropy due

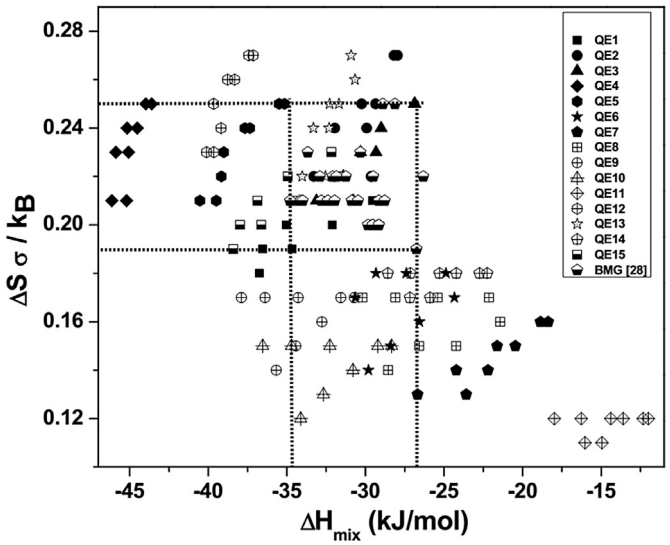

Fig. 3. ΔH_{mix} and $\Delta S_\sigma/k_B$ values for modeled quinary alloys (QE1 – QE15).

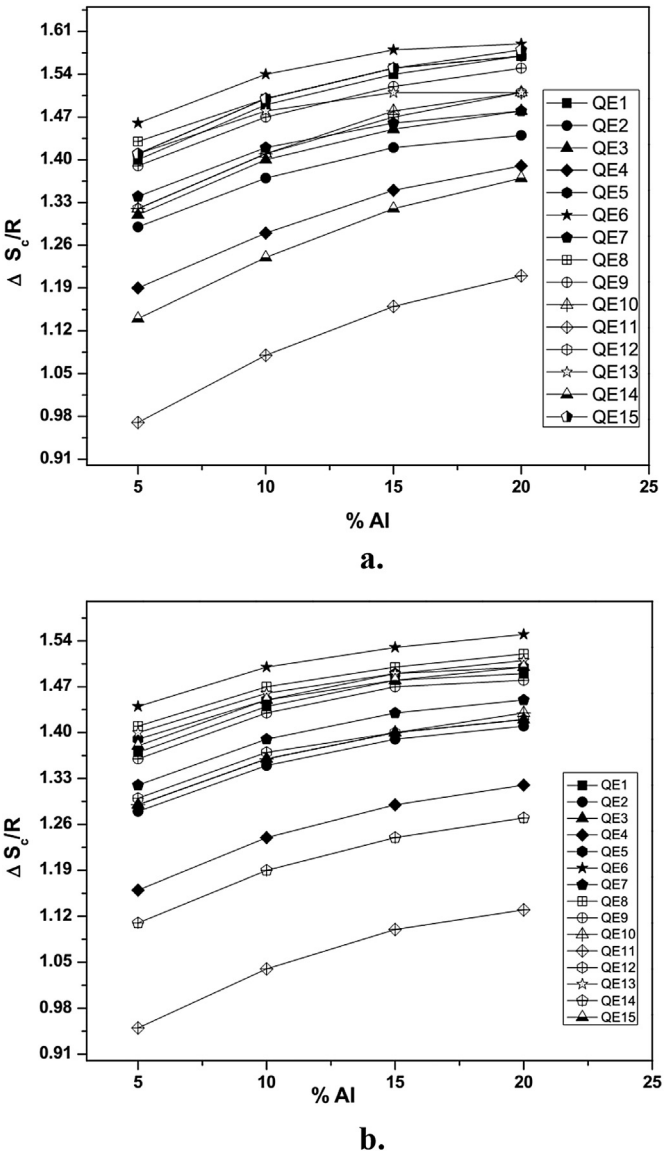

Fig. 4. $\Delta S_c/R$ variation with concentration of Al for (a) mode I and (b) mode II substitution.

to greater atomic size mismatch that existed due to large difference in atomic size between either Zr and Cu and Zr and Ni in the initial quaternary eutectic compositions. From Fig. 2a and b it can be concluded that Zr–Cu and Zr–Ni rich regions have greater mismatch entropy in comparison to alloys that are rich in Ti and Cu.

It is obvious that both Zr–Cu and Zr–Ni rich alloys possess more negative ΔH_{mix} and greater $\Delta S_\sigma/k_B$ in comparison to other alloys in this quinary system. However, the distinct boundaries of these parameters that result in BMG formation in Zr–Ti–Cu–Ni–Al system is still unclear. Hence in order to obtain more accurate estimate of the ΔH_{mix} and $\Delta S_\sigma/k_B$ range, these parametric values have been computed (Table 1) for the BMGs that have been reported in literature. Fig. 3 represents the plot of ΔH_{mix} against $\Delta S_\sigma/k_B$ for all the QEs and the BMGs reported in Zr–Ti–Cu–Ni–Al system (Table 1). All the reported BMGs occupy a distinct ΔH_{mix} range of −35 to −27 kJ/mol and $\Delta S_\sigma/k_B$ range of 0.19–0.25 as depicted in Fig. 3. For illustration of the BMG forming range, a window encompassing all the BMGs is drawn by erecting parallel lines through both the ΔH_{mix} and $\Delta S_\sigma/k_B$ axes (Fig. 3).

Interestingly, all the QE 3 compositions (Zr–Cu rich) lie within the window of BMGs (Table 2 in supplementary data). The origin for the excellent GFA of Zr–Cu rich alloys in Zr–Ti–Cu–Ni–Al system has been reported to be their proximity to deepest eutectics having invariant equilibrium temperatures less than 800 °C [31]. Allen et al. [32] reported that melts near deep eutectic regions in an alloy system have high degree of short range ordering (SRO) and also attractive potential between unlike atoms which ultimately result into large negative enthalpy of mixing and negative excess entropy. Multi-component alloys that satisfy the Inoue's empirical rules belong to the domain of deep eutectic regions which enhance the dense random packed structure and viscosity of super cooled liquid [33]. These regions are conducive for glass formation as they augment the solid–liquid interfacial energy to subdue the nucleation and growth of a crystalline phase [33]. However, in Fig. 3 apart from Zr–Cu rich QE 2 and QE 3 alloys, some Zr–Ti rich (QE 1), Ni–Cu rich (QE 13) and Zr rich (QE 15) (supplementary data) alloys also occupy the window of BMGs.

The GFA of QE 1, QE13 and QE 15 alloys occupying the window of BMGs (Fig. 3) needs further investigation as they represent composition regime different to Zr–Cu regions. QE 1 and QE 15 alloys have atomic concentration of Ti ranging from 15.8 to 20 at % and 13.5 to 17 at %, respectively, (Table 1 and Table 15 in supplementary data) which is higher in comparison to all the reported BMGs (Table 1 in supplementary data). GFA of Zr rich compositions in the current quinary system are very sensitive to Ti concentration, and it has been reported that only the Ti concentration within 2–3.7 at % stabilizes icosahedral order in the melt [34]. The adverse impact of substituting Ti beyond 2.6 at % on GFA in $Zr_{47.8}Cu_{32.8}Ni_{8.7}Al_{10.7}$ alloy has also been reported by Cao et al. [31] as it increases the liquidus temperature. Ti has ΔH_{mix} of +0.2 kJ/mol with Zr [26], hence alloys in Zr–Ti rich regime might induce phase separation leading to decreased GFA. QE 13 sequence of alloys (Table 13 in supplementary data) might have tendency for phase separation as these alloys are richer in Ni–Cu.

Singh et al. [35] proved experimentally that HEAs containing large difference in mixing enthalpies are prone to spinodal decomposition. There exist reports in the literature as to how the presence of elements with positive enthalpy of mixing induce phase separation and decrease GFA [36,37]. Kyeong et al. [38] demonstrated that alloying an element with positive enthalpy of mixing to a BMG composition can result into diverse amount of

Table 1
Computed P_{HSS} values of experimentally verified BMGs.

Composition	ΔH_{mix} kJ/mol	$\Delta S_\sigma/k_B$	$\Delta S_c/R$	P_{HSS} kJ/mol	Critical dia (Φ) mm [31]
$Zr_{52.5}Ti_5Ni_{14.6}Cu_{17.9}Al_{10}$	−33.67	0.23	1.31	−10.03	10
$Zr_{57}Ti_5Ni_8Cu_{20}Al_{10}$	−29.54	0.20	1.22	−7.34	10
$Zr_{54.5}Ti_{7.5}Ni_8Cu_{20}Al_{10}$	−29.15	0.20	1.28	−7.49	8
$Zr_{53}Ti_5Ni_{12}Cu_{20}Al_{10}$	−32.09	0.22	1.29	−9.25	8
$Zr_{60}Ti_{2.5}Ni_{10}Cu_{20}Al_{7.5}$	−29.50	0.22	1.15	−7.30	2.5
$Zr_{57.5}Ti_{2.5}Ni_{10}Cu_{20}Al_{10}$	−31.25	0.22	1.19	−8.02	2.5
$Zr_{55}Ti_{2.5}Ni_{10}Cu_{20}Al_{12.5}$	−32.81	0.21	1.23	−8.66	2.5
$Zr_{52.5}Ti_{2.5}Ni_{10}Cu_{20}Al_{15}$	−34.16	0.21	1.27	−9.22	2.5
$Zr_{57.5}Ti_5Ni_{10}Cu_{20}Al_{7.5}$	−29.15	0.21	1.21	−7.57	2.5
$Zr_{55}Ti_5Ni_{10}Cu_{20}Al_{10}$	−30.87	0.21	1.27	−8.33	2.5
$Zr_{52.5}Ti_5Ni_{10}Cu_{20}Al_{12.5}$	−32.39	0.21	1.30	−8.93	2.5
$Zr_{55}Ti_{7.5}Ni_{10}Cu_{20}Al_{7.5}$	−28.78	0.21	1.27	−7.74	2.5
$Zr_{52.5}Ti_{7.5}Ni_{10}Cu_{20}Al_{10}$	−30.47	0.21	1.32	−8.45	2.5
$Zr_{50}Ti_{7.5}Ni_{10}Cu_{20}Al_{12.5}$	−31.96	0.21	1.35	−9.04	2.5
$Zr_{57}Ti_5Ni_8Cu_{20}Al_{10}$	−29.54	0.20	1.22	−7.34	5
$Zr_{59}Ti_3Ni_8Cu_{20}Al_{10}$	−29.84	0.20	1.17	−7.12	3
$Zr_{53.1}Ti_{5.4}Ni_{11.7}Cu_{19.8}Al_{10}$	−31.85	0.22	1.30	−9.08	5
$Zr_{51.92}Ti_{5.28}Ni_{11.44}Cu_{19.36}Al_{12}$	−32.90	0.22	1.32	−9.40	5
$Zr_{50.56}Ti_{5.14}Ni_{11.14}Cu_{18.85}Al_{14.3}$	−34.00	0.21	1.33	−9.66	5
$Zr_{49.56}Ti_{5.04}Ni_{10.92}Cu_{18.48}Al_{16}$	−34.79	0.21	1.35	−9.78	5
$Zr_{51}Ti_5Ni_{10}Cu_{25}Al_9$	−30.32	0.23	1.29	−9.01	14
$Zr_{47.9}Ti_{0.3}Ni_{3.1}Cu_{39.3}Al_{9.4}$	−28.12	0.25	1.07	−7.40	9
$Zr_{57.1}Ti_{0.4}Ni_{3.5}Cu_{30.7}Al_{8.3}$	−27.37	0.22	1.03	−6.20	9
$Zr_{44.8}Ti_{0.2}Ni_{4.7}Cu_{40}Al_{10.3}$	−28.90	0.25	1.12	−8.13	9
$Zr_{59.3}Ti_{2.4}Ni_{2.6}Cu_{26.3}Al_{9.5}$	−26.75	0.19	1.07	−5.49	7

heterogeneity in the glass matrix depending upon the overall combination of ΔH_{mix} among the constituent elements. On the contrary, Wang et al. [39] reported that the presence of local crystalline ordering is responsible for enhancing GFA of Cu–Zr–Al alloy on 2 at % Y addition that has positive ΔH_{mix} with Zr.

From the preceding arguments it can be concluded that, the presence of elements with positive enthalpy of mixing in an alloy can either degrade GFA through phase separation or enhance GFA (when element that has positive mixing enthalpy is micro alloyed) through formation of local order that reduces the thermodynamic driving force for crystallization. The magnitude of positive ΔH_{mix} and concentration of the element that causes repulsive interaction with the solvent element decides whether the occurrence of phase separation or enhancement of GFA takes place. Hence while designing alloy compositions for glass formation; identification of regions that are richer in elements with positive ΔH_{mix} can simplify the quest for glass formers through elimination of those regions. In Zr–Ti–Cu–Ni–Al system Ni–Cu pair has the largest positive ΔH_{mix} followed by Zr–Ti pair. Hence the regions richer in these pair of elements might not be favorable for HEBMG formation. In view of the above criteria, QE 2 and QE 3 alloys are the probable HEBMG compositions in this entire quinary system.

The composition design for HEBMG is based on the idea that equiatomic/near equiatomic configuration of atoms favor configurationally disordered phases. Sluggish diffusion effect has been attributed to be the prime reason in an equiatomic alloy to form disordered structures, and it has been experimentally proved by Tsai et al. [40]. As the sluggish diffusion of atoms leads to high viscosity of a metallic liquid, it is envisaged that glass formation is stabilized due to high configurational entropy. Hence in order to understand the effect of configurational entropy on glass formation, the configurational entropy of all the alloys is calculated for two modes of substitution in all QEs (mode I and mode II) (Tables 1–15 in supplementary data) and the same is represented in Fig. 4a and b respectively. It is evident from Fig. 4a and b that configurational entropy of all the quinary compositions increases with increment in Al concentration. Apart from QEs 4, 11 and 14 all other QE series alloys are grouped between $\Delta S_c/R$ range of 1.3–1.5. As the $\Delta S_c/R$ for a quinary equiatomic alloy is 1.61 according to equation (8), most of the quinary modeled alloys in the current work are near to high configurational entropy regime and have the potential to form disordered phases.

The effect of configurational entropy in stabilizing glassy phase needs to be evaluated through the topology and population distribution of atomic clusters, since $\Delta S_c/R$ determines number of possible configurations of atomic arrangements. The topology of clusters is commonly determined by Voronoi polyhedra [41] generated through molecular dynamics simulations. Though the current work is not intended to determine the topology of the atomic clusters in Zr–Ti–Cu–Ni–Al system, certain qualitative comments can be made on the effect that configurational entropy exerts on GFA based on clusters reported in binary and ternary systems within the current quinary system. Wang and Wong [42] carried out MD simulations on wide compositional range in Cu–Zr–Al system and found that the population of clusters of higher coordination number (CN 13, 14, 15 and 16) have been found to gradually increase at the expense of lower coordination number clusters (CN 10, CN 11 and CN 12) with increase in Zr concentration from 20 to 70 at %.

The results are intuitive since, Zr has larger atomic diameter (0.3206 nm) in comparison to Cu (0.2556 nm) and has higher coordination number based on the radius ratio criterion of Miracle and Sanders [43]. In a similar work, Hui et al. [44] reported the origin of excellent GFA in Vit1 alloy to be the dominant icosahedra population along with wide range of coordination clusters from CN 9 to CN 16 whose fraction of population has been found to be in Gaussian distribution. From Hui et al. [44], it has been noticed that the fraction of clusters between CN 12 and CN 16 accounted to be 66%. Since Zr is the dominant element with 41.2 at % concentration in Vit 1 alloy, it resulted in clusters with higher coordination numbers like the case of Zr rich ternary Cu–Zr–Al alloys [42].

The above reports have probable relevance pertaining to atomic cluster distribution of the reported BMGs in Zr–Ti–Cu–Ni–Al system. To the best of the author's knowledge there exists no report that clarified the topology of atomic clusters through MD simulations in the alloy system under study. However, it is hypothesized

that BMGs in Table 1 have large fraction of atomic clusters with higher coordination number since Zr is the dominant element in these BMGs similar to those reported in Refs. [42,44]. Though it is undeniable that the majority of alloys modeled in this work have higher configurational entropy, the difference between glass forming alloys and non-glass formers lies in the stability and spatial connectivity of polyhedra when subjected to thermal fluctuations. The authors are of the firm opinion that stability of the SRO for various topological configurations during super-cooling and its ability to preserve icosahedral clusters through inter cluster sharing governs the dynamics of glass formation.

Hence the ability of interconnected atomic clusters to resist crystallization will be superior at a specific configuration of atoms among various available configurations. Zr rich regions in ETM-LTM-metalloid combination seem to have high GFA as they might make structural reorganization difficult due to high activation energy for atomic diffusion. The specific configuration of atoms where crystallization is difficult is facilitated by a particular range of negative enthalpy of mixing and atomic size differences among the constituent elements of the alloy. Hence there seem to have a strong connection between negative enthalpy of mixing, atomic size difference and configurational entropy which interact in complex manner to stabilize glass.

To correlate the simultaneous effect of all above three parameters, the P_{HSS} range for each QE is captured through box plot in Fig. 5 which allows comparison of range and variance of P_{HSS} for QEs 1–15 with that of BMGs (Table 1). The dashed lines depict the window of P_{HSS} for BMG formation. As seen from the box plot, the P_{HSS} for BMG formation is within the range of −10 to −5 kJ/mol. However, the mean value of P_{HSS} for BMG is around −8.0 kJ/mol. Since most of BMGs lie within the P_{HSS} range between −7.4 kJ/mol (75th percentile value) and minimum value (−10 kJ/mol), this range is proposed to be the window for BMG formation within this system. The box plot can be divided into three regions based on the P_{HSS} range. P_{HSS} range of −8 to −1 kJ/mol where probability of glass formation is very limited due to suboptimal enthalpy, topology and configurational entropy parameters, −10 to −8 kJ/mol region which is conducive for BMG formation and third region where P_{HSS} is less than −10 kJ/mol is prone to formation of intermetallic phases.

Hence, $Zr_{33}Ti_9Cu_{34}Ni_9Al_{15}$ alloy, a representative of QE 3 alloys which has a ΔH_{mix} and a $\Delta S_\sigma/k_B$ of −30.31 kJ/mol, and 0.23 respectively (similar to 14 mm glass former) and a $\Delta S_c/R$ of 1.45 (Table 3 in supplementary data) is proposed to be a HEBMG

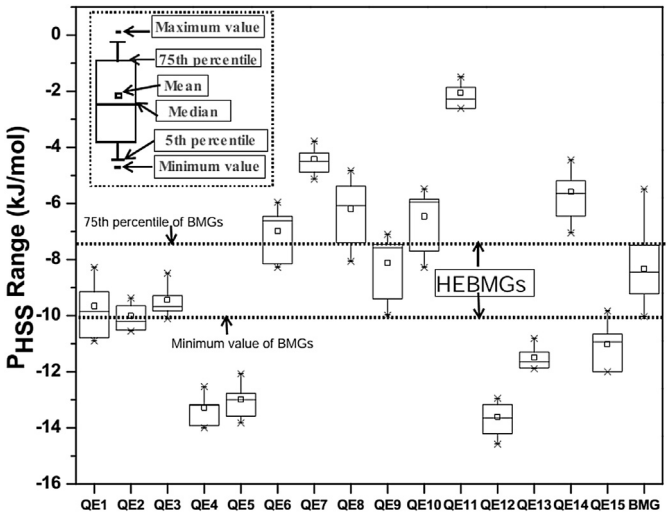

Fig. 5. P_{HSS} of modeled quinary alloys (QE1 − QE15).

(though it is not an equiatomic alloy, this alloy is referred to as HEBMG because it has large $\Delta S_c/R$ almost near to 1.5) [45]. In addition to the above alloy, certain other compositions in QE 2 and QE 3 are also anticipated to be medium entropy BMGs (Table 2) as their $\Delta S_c/R$ lies between 1.37 and 1.45. There exists a strong probability that an alloy composition within the regime of the alloys (Table 2) might have higher GFA than the reported BMGs. To pin point this composition, metallographic approach adopted by Wang et al. [46] through monitoring the microstructure of the alloys is a promising method. Furthermore, the P_{HSS} of equiatomic Zr–Ti–Cu–Ni–Al is calculated and found to be −10.48 kJ/mol (ΔH_{mix} of −34.26 kJ/mol, $\Delta S_\sigma/k_B$ of 0.19 and $\Delta S_c/R$ of 1.61). $Zr_{30}Ti_{23}Cu_{15}Ni_{22}Al_{10}$ alloy with P_{HSS} of −11.36 kJ/mol (ΔH_{mix} of −34.33 kJ/mol, $\Delta S_\sigma/k_B$ of 0.21 and $\Delta S_c/R$ of 1.57) has been reported to form amorphous ribbon (Φ 0.7 mm) by Czeppe et al. [47]. In the same report [47] $Zr_{34.5}Ti_{23}Cu_{12.5}Ni_{22}Al_8$ alloy with P_{HSS} of −11.06 kJ/mol (ΔH_{mix} of −34.15 kJ/mol, $\Delta S_\sigma/k_B$ of 0.21 and $\Delta S_c/R$ of 1.54) has been reported to form Zr_2Ni phase.

5.2. Experimental results

The amorphous phase evolution as function of milling time for certain QE9 (two compositions), QE3 and QE2 alloys is depicted in Figs. 6–9. In line with the hypothesis proposed through P_{HSS} modeling, Z1 and Z2 alloys that belong to QE3 and QE2 alloy series display good GFA in comparison to T1 and T2 alloys of QE9 series as evident from XRD patterns (Figs. 6–9). QE2 and QE3 alloys display significant amorphous phase formation after 6 h of ball milling which is not the case for QE 9 alloys. After 6 h of ball milling Ti–Ni rich QE9 alloys contain significant fraction of nano crystalline phases in amorphous matrix as noticed from diffractograms. Furthermore, GFA of Z2 alloy is better than Z1 alloy and this is attributed to less Ti concentration as reported in literature [34].

As discussed earlier, increasing concentration of Ti and Ni and decreasing Zr and Cu concentration favors Zr_2Ni phase and hence the alloys suggested as HEBMGs in Table 2 have both the Ti and Ni less than the composition that formed amorphous ribbon reported by Czeppe et al. [47]. The current work could not resolve as to why QE1 and QE9 compositions (Fig. 5) and equiatomic Zr–Ti–Cu–Ni–Al (not shown in Fig. 5) cannot form BMGs of optimum GFA despite their presence in the arbitrary window of BMG formation. This can be attributed to the non-incorporation of kinetic parameters that account for structural relaxations and phenomenon like liquid–liquid phase transition for estimating glass formation. A lot of further research scope is envisaged in this direction to modify P_{HSS} parameter based on kinetic perspectives that aims to obviate the anomalies mentioned in previous discussion. In the report of Czeppe et al. [47] both the Al doped alloys mentioned above, are in high configurational entropy domain and almost similar composition and P_{HSS} values but one forms amorphous ribbon (Φ 0.7 mm) and the other forms intermetallic (Zr_2Ni) phase. It is the inherent limitation of the current thermodynamic model that certain intermetallic phases and BMGs have similar P_{HSS}

Table 2
List of proposed HEBMGs in this work.

Composition	ΔH_{mix} kJ/mol	$\Delta S_\sigma/k_B$	$\Delta S_c/R$	P_{HSS} kJ/mol
$Zr_{34.8}Ti_{5.1}Cu_{37.9}Ni_{12.2}Al_{10}$	−29.35	0.25	1.37	−10.20
$Zr_{29.8}Ti_{5.1}Cu_{37.9}Ni_{12.2}Al_{15}$	−29.92	0.24	1.42	−10.08
$Zr_{43.5}Ti_{7.6}Cu_{30.4}Ni_{8.5}Al_{10}$	−29.33	0.23	1.36	−9.29
$Zr_{41.1}Ti_{7.2}Cu_{28.7}Ni_8Al_{15}$	−31.41	0.22	1.40	−9.72
$Zr_{38.3}Ti_{8.5}Cu_{33.8}Ni_{9.4}Al_{10}$	−29.00	0.24	1.40	−9.68
$Zr_{33}Ti_9Cu_{34}Ni_9Al_{15}$	−30.31	0.23	1.45	−10.11
$Zr_{28.3}Ti_{8.5}Cu_{33.8}Ni_{9.4}Al_{20}$	−30.78	0.21	1.48	−9.64

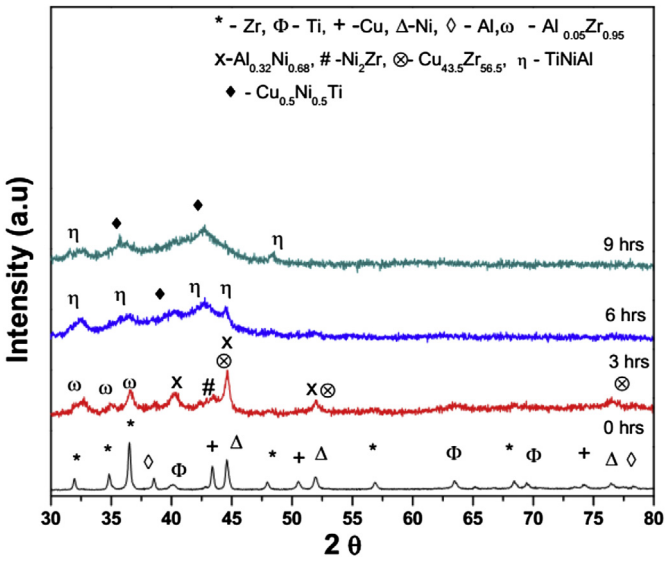

Fig. 6. XRD pattern for $Zr_{15.2}Ti_{37.4}Cu_{10.4}Ni_{27}Al_{10}$ (T1) composition.

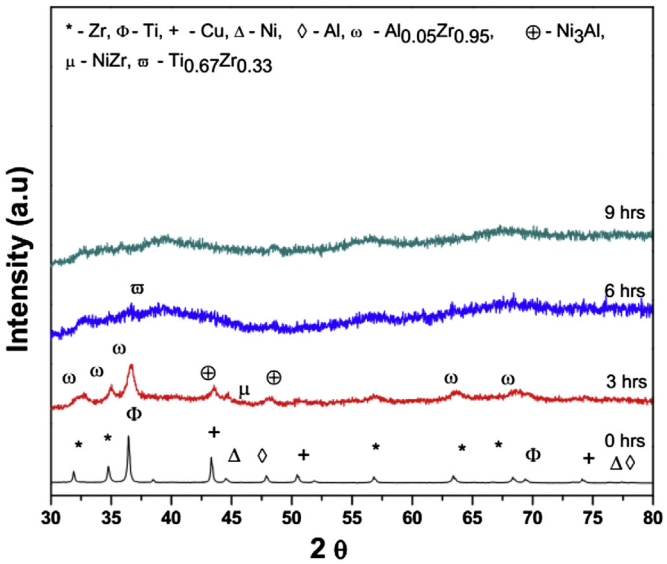

Fig. 8. XRD pattern for $Zr_{43.5}Ti_{7.6}Cu_{30.4}Ni_{8.5}Al_{10}$ (Z1) composition.

values. Moreover, the trend of P_{HSS} values is inconsistent with critical diameter (Φ) and discrepancies in Φ can be observed for compositions having similar P_{HSS} (Table 1). It can be attributed to the lack of current understanding as to how the thermodynamic and topological parameters influence the cluster dynamics in glass formation.

Though an optimum window of these parameters has been established in the current study, how different compositions having equal P_{HSS} obtained through different combination of ΔH_{mix}, $\Delta S_\sigma/k_B$ and $\Delta S_c/R$ influence GFA can only be understood through visualization of their atomic clusters from MD simulations. Moreover, understanding the functional relationship between the thermodynamic parameters used in this work with atomic clusters can bridge the gap between the classical thermodynamic methods and currently popular Voronoi clusters depicted by MD simulations. Such a thorough understanding enables perspicuous comprehension behind the mechanism of glass formation in metallic alloys.

This study on GFA of Zr–Ti–Cu–Ni–Al system in high entropy regime is based on Takeuchi's approach of capturing optimum window for glass formation as discussed in introductory section. Adopting this approach near eutectic regions of Zr–Ti–Cu–Ni quaternary system facilitated to screen down the potential compositions for HEBMG based on simple thermodynamic calculations. Despite simplified assumptions like neglecting higher order interaction parameters in calculating the mixing enthalpies of the alloys and also assuming atoms as hard spheres, our results establish strong correlation of thermodynamic and topological requirements between experimentally established BMGs and modeled alloys in the Zr–Cu rich region of this quinary system. Composition optimization near eutectic regions using P_{HSS} parameter proves that deep eutectic regions are necessary but not sufficient criteria for glass formation. Only the alloys that have optimum chemical interaction and assure dense random packing near eutectic regions can form glasses.

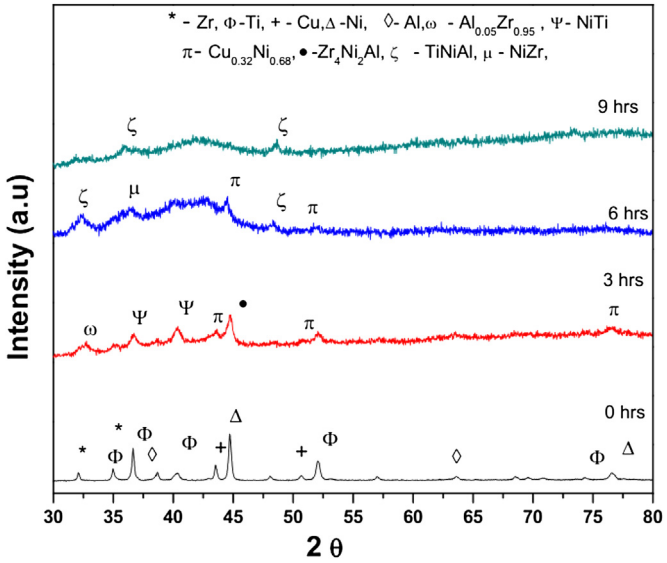

Fig. 7. XRD pattern for $Zr_{14.4}Ti_{45.1}Cu_{9.9}Ni_{25.6}Al_5$ (T2) composition.

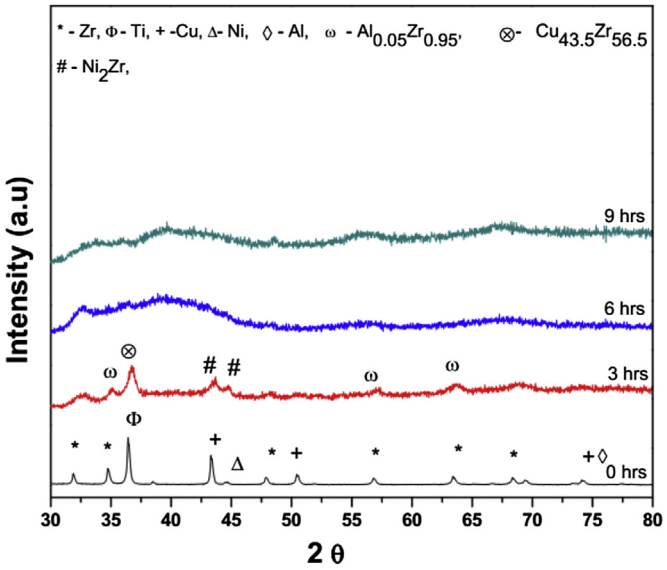

Fig. 9. XRD pattern for $Zr_{40.3}Ti_{4.6}Cu_{34.1}Ni_{11}Al_{10}$ (Z2) composition.

6. Conclusions

a) The present work identified a window of P_{HSS} values for easy glass formation. High entropy alloy philosophy of alloy design simplifies the complexity in discovering novel glass forming compositions. P_{HSS} parameter is effective to locate that not all deep eutectic regions are conducive for glass formation.
b) Takeuchi's approach of capturing optimum window for glass formation based on two dimensional plot of mixing enthalpy and mismatch entropy can be applied to other HEAs towards screening down compositions for HEBMG formation.

Appendix A. Supplementary data

Supplementary data related to this article can be found at http://dx.doi.org/10.1016/j.intermet.2015.04.007.

References

[1] Klement W, Willens RH, Duwez P. Nature 1960;187:869–70.
[2] Cheng YQ, Ma E. Prog Mater Sci 2011;56:379–473.
[3] Ashby MF, Greer AL. Scr Mater 2006;54:321–6.
[4] Kumar G, Desai A, Schroers J. Adv Mater 2011;23:461–76.
[5] Inoue A, Takeuchi A. Acta Mater 2011;59:2243–67.
[6] Wang H, Park ES, Oak JJ, Setyawan AD, Zhu SL, Wada T, et al. J Non-Cryst Sol 2013;379:155–60.
[7] Zhao K, Xia XX, Bai HY, Zhao DQ, Wang WH. Appl Phys Lett 2011;98:141913 (1-3).
[8] Wang WH. JOM 2014;66:2067–77.
[9] Gao XQ, Zhao K, Ke HB, Ding DW, Wang WH, Bai HY. J Non-Cryst Sol 2011;357:3557–60.
[10] Ding HY, Shao Y, Gong P, Li JF, Yao KF. Mater Lett 2014;125:151–3.
[11] Takeuchi A, Chen N, Wada T, Yokoyama Y, Kato H, Inoue A, et al. Intermetallics 2011;19:1546–54.
[12] Zhang F, Zhang C, Chen SL, Zhu J, Cao WS, Kattner UR. Calphad 2014;45:1–10.
[13] Jones NG, Frezza A, Stone HJ. Mater Sci Eng A 2014;615:214–21.
[14] Takeuchi A, Inoue A. Mater Trans 2000;41:1372–8.
[15] Yun YS, Nam HS, Cha PR, Kim WT, Kim DH. Met Mater Int 2014;20:105–11.
[16] Takeuchi A, Amiya K, Wada T, Yubuta K, Zhang W, Makino A. Entropy 2013;15:3810–21.
[17] Takeuchi A, Amiya K, Wada T, Yubuta K, Zhang W, Makino A. Mater Trans 2014;55:165–70.
[18] Yang X, Zhang Y. Mater Chem Phys 2012;132:233–8.
[19] Guo S, Hu Q, Ng C, Liu CT. Intermetallics 2013;41:96–103.
[20] Ma D, Cao H, Chang YA. Intermetallics 2007;15:1122–6.
[21] Lee DM, Sun JH, Kang DH, Shin SY, Welsch G, Lee CH. Intermetallics 2012;21:67–74.
[22] Cheng YQ, Ma E, Sheng HW. Phys Rev Lett 2009;102:245501 (1-4).
[23] Gallego LJ, Somoza JA, Alonso JA. J Phys Condes Mat 1990;2:6245–50.
[24] Murty BS, Ranganathan S, Rao MM. Mat Sci Eng A 1992;149:231–40.
[25] Niessen AK, de Boer FR, Boom R, de Chatel PF, Mattens WCM, Miedema AR. Calphad 1983;7:51–70.
[26] Takeuchi A, Inoue A. Intermetallics 2010;18:1779–89.
[27] Mansoori GA, Carnahan NF, Starling KE, Leland Jr TW. J Chem Phys 1971;54:1523–5.
[28] Senkov ON, Miracle DB. Mater Res Bull 2001;36:2183–98.
[29] RamaKrishna Rao B, Srinivas M, Shah AK, Gandhi AS, Murty BS. Intermetallics 2013;35:73–81.
[30] Xing D, Shen J, Zhang L, Sun J, Wang X, Wang H, et al. J Alloy Compd 2009;481:531–8.
[31] Cao H, Ma D, Hseih KC, Ding L, Stratton WG, Voyles PM, et al. Acta Mater 2006;54:2975–82.
[32] Allen JW, Wright AC, Connell GAN. J Non-Cryst Solids 1980;42:509–24.
[33] Inoue A. Acta Mater 2000;48:279–306.
[34] Kuhn U, Eymann K, Mattern N, Eckert J, Gebert A, Bartusch B, et al. Acta Mater 2006;54:4685–92.
[35] Singh S, Wanderka N, Murty BS, Glatzel U, Banhart J. Acta Mater 2011;59:182–90.
[36] Mattern N, Vainio U, Park JM, Han JH, Shariq A, Kim DH, et al. J Alloy Compd 2011;509S:S23–6.
[37] Han JH, Mattern N, Schwarz B, Kim DH, Eckert J. Scr Mater 2012;67:149–52.
[38] Kyeong JS, Kim DH, Lee JI, Park ES. Intermetallics 2012;31:9–15.
[39] Wang Q, Liu CT, Yang Y, Liu JB, Dong YD, Lu J. Sci Rep 2014;4:1–5.
[40] Tsai KY, Tsai MH, Yeh JW. Acta Mater 2013;61:4887–97.
[41] Voronoi G, Reine J. Angew Math 1908;134:198–287.
[42] Wang CC, Wong CH. J Alloy Compd 2012;510:107–13.
[43] Miracle DB, Sanders WS. Philos Mag 2003;83:2409–28.
[44] Hui X, Fang HZ, Chen GL, Shang SL, Wang Y, Qin JY, et al. Acta Mater 2009;57:376–91.
[45] Murty BS, Yeh JW, Ranganathan S. High entropy alloys. Butterworth-Heinemann; 2014.
[46] Wang D, Tan H, Li Y. Acta Mater 2005;53:2969–79.
[47] Czeppe T, Rashkova V, Dobrev E, Litynska L, Morgiel J, Labar JL, et al. Mat Sci Eng A 2004;375–377:260–4.